tions in chlorodifluoromethane and in dimethyl ether (130-150 mg in 2.2. mL of solution) containing 18% of CD_2Cl_2 (for locking purpose) and a small quantity of Me_4Si in 10-mm tubes which had degassed and sealed. The following instrumental parameters are typical: flip angle = 60-90°; SW = 20 000 Hz; data size = 16 K or data points and acquisition time = 0.41 s; number of scans = 500-2000; power decoupler (attenuation 5 dB on high range of the standard decoupler). The NMR data were treated by an exponential multiplication with LB varying from 1 to 6. A delay of 0.1-0.2 s was added between pulses for the spectra used for integration.

The rate constants were determined at the coalescence temperature by using the equation $k = \pi\Delta\nu/\sqrt{2}$ for singlet to doublet splitting in ^{13}C NMR spectra; this equation is known to give acceptable approximation even in the case of lines of unequal intensities.[12,15] The equation $k = \pi(\Delta\nu^2 + 6J^2)^{1/2}/\sqrt{2}$ was used for singlet to AB ^1H NMR spectral change. The free-energy barriers ($\Delta G^\ddagger$) were calculated from standard equations by using a transmission coefficient of $^1/_2$ or 1 one (vide infra).

Determinations of activation parameters of **7** were done by calculation of spectra at low temperature by using a slightly modified version of the DNMR-2 program on a CDC Cyber 173 computer.[1] The simulations were done by a visual comparison of the calculated and experimental spectra. Free energies of activation were calculated from a $\ln k/T$ vs. $1/T$ plot by using the Eyring equation.[15] Calculations of $\Delta S^\ddagger$ and $\Delta H^\ddagger$ were carried out from rate data obtained at several temperatures. The complete treatment was carried out by using standard procedures.[15] The two-dimensional ^1H NMR COSY experiment[8] was carried out with the standard Bruker 2D software and equipment by using the following pulse sequence: RD-90°-t_1-90°-t_2 (F1D). A spectral width of 2500 Hz and quadrature detection were used to collect a 128 F1D × 2K data matrix by using 16 scans. Zero filling gave a 1K × 2K matrix affording a digital resolution of 2.44 Hz/Pt. A sine bell square function was applied in both dimensions and absolute display was used.

1,3,4,5-Tetrahydro-2-Benzoxepin (6). This compound was prepared by using the method described by Rieche and Gross.[30] The procedure was slightly modified as follows: the intermediate chloromethyl 3-phenylpropyl ether was not distilled but conserved by adding some $CaCl_2$ as drying agent. In our hands heating led to apparent dimerization. The product was flash chromatographed on silica gel[31] and characterized as follows: ^1H and ^{13}C NMR spectra (Figure 2, Table II); mass spectrum EI; calcd for $C_{10}H_{12}O$ 148.0888, found 148.0885.

3-Methoxy-1,3,4,5-Tetrahydro-2-Benzoxepin (7). Compound **7** was prepared as previously described.[7] Its ^1H NMR was found to be identical with that reported, and the ^{13}C NMR spectrum (Figure 2 and Table I) confirms its identity.

Acknowledgment. We acknowledge the assistance of Dr. M. T. Phan Viet, mananger of the "Laboratoire Régional de RMN á haut champ" in Montréal. We are thankful for financial assistance from the Natural Sciences and Engineering Research Council of Canada.

Registry No. 6, 5698-85-1; **7**, 87751-23-3; **8**, 6581-66-4.

(30) Rieche, A.; Gross, H. *Chem. Ber.* **1961**, *95*, 91.
(31) Still, W. C.; Kahn, M.; Nitra, A. *J. Org. Chem.* **1978**, *43*, 2923.

Surface Site Distributions by Solid-State Multinuclear NMR Spectroscopy. Pyridine Binding to γ-Alumina by ^{15}N and ^2H NMR

Paul D. Majors and Paul D. Ellis*

Contribution from the Department of Chemistry, University of South Carolina, Columbia, South Carolina 29208. *Received August 25, 1986*

Abstract: The surface preparation dependent interactions of pyridine with γ-alumina are explored with solid-state ^{15}N and ^2H NMR spectroscopies. The observation of pyridine-^{15}N adsorbed to the surface reveals two resonances which are both characteristic of pyridine participating in a Lewis acid-base complex. These resonances display only partial tensorial averaging, and full information about the motionally averaged tensors is derived from magic angle spinning sideband simulations. Both resonances are assigned to complexes containing coordinatively unsaturated surface aluminum cations which occupy tetrahedral and octahedral sites in the defect spinel lattice. The relative distributions of tetrahedral and octahedral Lewis acid sites are determined as a function of surface preparation conditions, and the results are used with a simple surface preparation model to calculate the relative contribution of the various low index lattice planes to the composition of the surface. ^2H NMR line-shape studies of pyridine-α,α'-d_2 on γ-alumina indicate a heterogeneous distribution of pyridine motional species, which reflect the physical and steric characteristics of the surface binding sites. Quadrupolar spin-echo line-shape simulations for various motional models indicate the significant contributions of pyridines undergoing continuous diffusion or twofold ring flips about their twofold symmetry axis.

In the past several years we have been interested in the application of modern multinuclear solid-state NMR methods to probe the interactions between a sorbate and alumina surfaces. Our initial work involved the application of ^{13}C NMR to the chemisorption of amines, e.g., *n*-butylamine[1] and pyridine[2] to γ-alumina. In response to our pyridine work Ripmeester[3] published an interesting paper describing his ^{15}N NMR experiments utilizing ^{15}N-enriched pyridine on γ-alumina. In that paper he reported that pyridine forms two distinguishable Lewis acid complexes with γ-alumina. This is clearly an important observation which demonstrates the importance of utilizing more than a single "nuclear spin-label" when studying systems as complicated as these.

The importance of this observation, in addition to the difference in methods of γ-alumina preparation, prompted us to confirm his observations. Indeed we do confirm his results. In addition, we have determined the individual elements of the shielding tensor for each of the sites. With these data we have postulated that the two ^{15}N resonances represent pyridine nitrogen atom coordination to tetrahedral and octahedral Al^{3+} sites on the surface of the γ-alumina. The surface preparation dependence of the relative contribution of these resonances to the ^{15}N NMR spectra was observed and used to analyze the surface acid site distribution and to discuss the possible structure of the surface. Finally, the

(1) Dawson, W. H.; Kaiser, S. W.; Ellis, P. D.; Inners, R. R. *J. Am. Chem. Soc.* **1981**, *103*, 6780.
(2) Dawson, W. H.; Kaiser, S. W.; Ellis, P. D.; Inners, R. R. *J. Phys. Chem.* **1982**, *86*, 867.
(3) Ripmeester, J. A. *J. Am. Chem. Soc.* **1983**, *105*, 2925-2927.

0002-7863/87/1509-1648$01.50/0 © 1987 American Chemical Society

motional heterogeneity of the Lewis site coordinated pyridine molecules as observed by solid-state ^{2}H NMR is discussed.

Experimental Section

Samples. The γ-alumina surface samples were prepared from carefully ground high-purity pellets (Norton catalyst support No. SA6173; 220 m^2/g). Individual 1.0-g samples were added to glass break-seal tubes (Pyrex or quartz), vacuum dried by various subsequently mentioned techniques, and flame sealed under vacuum. Three individual methods for vacuum drying the γ-alumina samples were employed. A partially dehydroxylated alumina (PDA) sample was prepared by evacuating the sample for 8 h at 350 °C to a final pressure of 10^{-5} torr. An intermediately dehydroxylated alumina (IDA) sample was prepared by evacuating the starting material at 510–550 °C, calcining the sample under O_2 for 30 min (3–10-min intervals with intermittent evacuation), and evacuating the surface for 3 h at 610 °C. An extensively dehydroxylated alumina (EDA) sample was obtained by calcining the starting material under O_2 for 1 h at 815 °C and evacuating for 5 h at the same temperature to an ultimate pressure of 10^{-6} torr.

To the other chamber of the break-seal tube, measured samples of purified pyridine-^{15}N or pyridine-α,α'-d_2[4] (dried over sodium metal or calcium hydride and then vacuum distilled) were measured (370 μmol corresponding with approximately 25% monolayer, where one monolayer is defined in this study as four molecules per 100 $Å^2$ surface) and flame sealed under vacuum. The adsorbent and adsorbate were united and equilibrated by shattering the break-seal and heating the break-seal tube at 120 °C for 1 h before slowly cooling to room temperature. The NMR samples were prepared just prior to the magic angle spinning (MAS) experiments by opening the break-seal tubes in a Vacuum Atmospheres drybox and packing the treated γ-Al_2O_3 into ceramic sample rotors (MAS NMR sample containers). These samples are stable to O_2 and H_2O for several days when spinning with dry N_2 gas.

Pyridine-α,α'-d_2 was prepared according to the method of Zoltewicz and Smith.[4] First, 2 mL of reagent grade pyridine was treated with 15 mL of D_2O and 2 drops of DCl in a heavy-walled glass tube for over 72 h at a temperature of 120 °C. The reacted pyridine was separated from water by extracting with two 20-mL portions of diethyl ether.

The bulk of the ether was removed from the pyridine by a simple distillation. The product was transferred to a vacuum line where it was dried over a generous amount of calcium hydride (approximately 200 mg). The product was degassed at liquid nitrogen temperature to remove all noncondensable gases and was next vacuum distilled at −20 °C (CCl_4 slush bath). A 90-MHz ^{1}H NMR spectrum of the product (neat) showed 95% deuteration at the α positions of pyridine, and also the presence of ether:pyridine in a ratio of approximately 2 to 1. The sample was again vacuum distilled, this time at −42 °C (pyridine slush bath), and retrieved for ^{1}H NMR analysis, this time to show only a trace of ether and water. The pyridine-α,α'-d_2 was dried over calcium hydride immediately before subsequent sample preparations, the purity being verified by ^{1}H NMR of the neat liquid.

^{15}N NMR spectra of pyridine-^{15}N on γ-Al_2O_3 were obtained with a Varian XL-300 spectrometer at a resonance frequency of 30.4 MHz utilizing a magic angle spinning probe purchased from Doty Scientific, Inc.[5] The techniques of cross-polarization,[6] magic angle spinning[7] with rotationally synchronized spin–echo refocusing of the magnetization, and high-power proton decoupling were employed. The recycle delay and cross-polarization times were optimized to ensure an accurate representation of relative spin density for all resonances. A series of surface hydration experiments were performed on a Bruker WH-400 spectrometer at a resonance frequency of 40.55 MHz. Additionally, a dipolar dephasing[8] experiment was performed to test for the presence of hydrogen bonding and/or direct association of hydrogen to the pyridine nitrogen.

Solid-state ^{2}H spectra were obtained on a Varian XL-400 spectrometer at a resonance frequency of 61.4 MHz. The NMR sample probe employed was a single-resonance 5-mm NMR powder probe purchased from Doty Scientific, Inc. A quadrupole spin–echo[9] pulse sequence was utilized for all ^{2}H experiments, and the experimental parameters were optimized using a perdeuterated polyethylene sample for a line-shape reference. Ninety degree pulse widths of 3.0 μs were attained with an ENI LPI-10 linear amplifier at 800 W of power. Subsequently only data leftshifting and zero-order phase correction were used to phase the spectra. We define the separation between the perpendicular edges (the "horns") of the powder pattern as $\omega_Q/2\pi$. This separation is 3/4 of the motionally averaged quadrupole coupling constant.

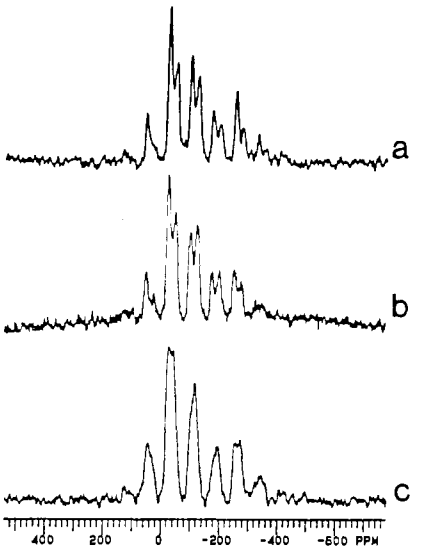

Figure 1. (a) 30.4-MHz ^{15}N CP/MAS spectra of pyridine-^{15}N on γ-alumina (25% monolayer surface coverage): (a) PDA sample, 12 160 1s is repetitions, 3-ms cross-relaxation time, ~2350 revolutions/s; (b) IDA sample, 25 025 1s repetitions, 3-ms cross-relaxation time, ~2330 revolutions/s; (c) EDA sample, 35 072 1s repetitions, 3-ms cross-relaxation time, ~2300 revolutions/s.

Table I. ^{15}N Chemical Shielding Tensor Elements for ^{15}N-Labeled Pyridine[a]

sample	site	$\bar{\sigma}$	δ	η	LWHM[b]	rel %[c]
PDA						
	1	−103	−255	0.29	16	61
	2	−124	−226	0.09	23	39
IDA						
	1	−106	−263	0.26	18	57
	2	−129	−222	0.20	20	43
EDA						
	1	−109	−226	0.17	20	51
	2	−123	−225	0.21	20	49
partial exposure to air		−110				
extended exposure to air		−78				

[a] Chemical shifts are reported in ppm relative to the nitrate resonance of NH_4NO_3 (0.1 M) via a secondary reference with polycrystalline NH_4NO_3; $\bar{\sigma} = (\sigma_{xx} + \sigma_{yy} + \sigma_{zz})/3$; $\delta = \sigma_{zz} - \bar{\sigma}$; $\eta = (\sigma_{yy} - \sigma_{xx})/\delta$. [b] LWHM = line width at half-maximum peak intensity (ppm). [c] Rel % is the percent distribution of the resonance to the spectrum.

Results and Discussion

The ^{15}N MAS spectra for ^{15}N-labeled pyridine on each of the γ-alumina surface preparations (PDA, IDA, EDA; Figure 1) show two resonances with isotropic shifts ranging from −103 to −109 ppm, and −123 to −129 ppm relative to the nitrate resonance of NH_4NO_3 (labeled Lewis sites 1 and 2, respectively, in Table I). These isotropic resonances correspond to the two Lewis acid site resonances observed in Ripmeester's ^{15}N NMR study[3] of γ-Al_2O_3 saturated with pyridine-^{15}N. A dipolar dephasing experiment confirms the inference from the chemical shielding values that neither of the two resonances represents a hydrogen-bonded or protonated species. This is in agreement with previous studies[10-12]

(4) Zoltewicz, J. A.; Smith, C. L. *J. Am. Chem. Soc.* **1967**, *89*, 3358.
(5) Doty, F. D.; Ellis, P. D. *Rev. Sci. Instrum.* **1981**, *52*, 1868–1875.
(6) Pines, A.; Gibby, M. G.; Waugh, J. S. *J. Chem. Phys.* **1973**, *59*, 569–590.
(7) (a) Lowe, I. J. *Phys. Rev. Lett.* **1975**, *2*, 285. (b) Andrew, E. R.; Bradbury, A.; Eades, R. G. *Nature (London)* **1958**, *182*, 1659.
(8) Opella, S. J.; Frey, M. H.; Cross, T. A. *J. Am. Chem. Soc.* **1979**, *101*, 5854–5856.
(9) Davis, J. H.; Jeffrey, K. R.; Bloom, M.; Valic, M. I.; Higgs, T. P. *Chem. Phys. Lett.* **1976**, *42*, 390.
(10) (a) Parry, E. P. *J. Catal.* **1963**, *2*, 371. (b) Knozinger, H.; Kaerlein, C. P. **1972**, *25*, 436. (c) Gay, I. D.; Liang, S. *Ibid.* **1976**, *44*, 306.
(11) Knozinger, H. *Adv. Catal.* **1976**, *25*, 184–271.
(12) (a) Knozinger, H.; Krietenbrink, H.; Muller, H.-D.; Schulz, W. *Proc. Int. Congr. Catal., 6th* **1977**, 183–194. (b) Knozinger, H.; Krientenbrink, H.; Ratnasamy, P.; *J. Catal.* **1977**, *48*, 436. (c) Corma, A.; Rodellas, C.; Fornes, V. *Ibid.* **1984**, *88*, 374.

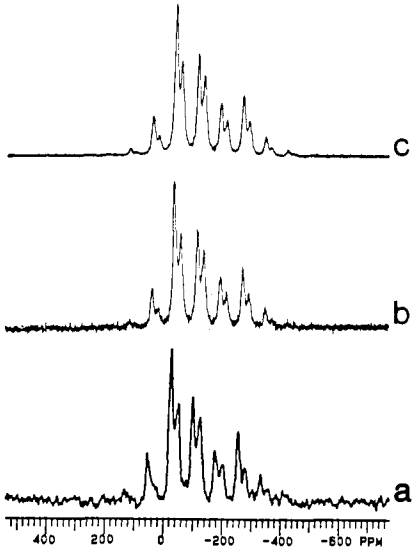

Figure 2. (a) 30.4-mHz ^{15}N CP/MAS spectrum of pyridine-^{15}N on γ-alumina (PDA surface; 25% monolayer surface coverage), 12 160 1s repetitions, 3-ms contact time, ~2350 revolutions/s. (b) Optimized spectral simulation with artificial noise. (c) Optimized spectral simulation.

which show that γ-alumina has insufficient Brønsted acidity to protonate the relatively weak base pyridine.

At the magnetic field strengths employed in this study (7.1 and 9.4 T) spinning sidebands from each of the Lewis acid sites can clearly be distinguished. Hence, by examining the spectra as a function of spinning speed one can readily deduce the values of δ and η (see Table I) and $\bar{\sigma}$ for each site. The isotropic shifts were also confirmed by performing a TOSS (total suppression of sidebands)[13] experiment (spectrum not shown). Optimized computer simulations[14] of the experimental MAS sideband patterns were generated in order to determine the anisotropy and the asymmetry parameter for each of the ^{15}N chemical shielding tensors. A representative simulation is shown in original form (Figure 2c) and with artificial noise applied before Fourier transformation of the simulated free induction decay (Figure 2b). These simulations were compared with the experimental spectra (Figure 2a), and the goodness of fit was evaluated by calculating the square of differences between the experimental and simulated spectral sideband intensities, weighting them by the experimental sideband intensities (i.e., the relative signal to noise ratio), and summing the values. The resulting value was used as a goodness of fit response for a variable size gradient search simplex optimization algorithm[15] which iteratively (and empirically) varies tensor parameters, executes the MAS simulation, and uses the response to choose the next set of parameters. When a stable optimum response is approached, the variation increment for the parameters decreases until it reaches a predefined convergence limit around the optimum value. For these spectral simulations, a five-parameter simplex optimization routine was employed (two tensors are to be defined, so two anisotropies, two asymmetry parameters, and one tensor ratio parameter are needed).

The ^{15}N shielding tensor parameters for the surface coordinated pyridines may be compared with those for solid pyridine. Schweitzer and Spiess[16] determined these values for pyridine at −105 °C: $\bar{\sigma}$ = −84 ppm (relative to aqueous 0.1 M NH_4NO_3), δ = −448 ppm, and η = 0.49. $\bar{\sigma}$, δ, and η are linear combinations of σ_{xx}, σ_{yy}, and σ_{zz}, which are the symmetric PAS (principal axis system) shielding tensor elements as defined in Table I. The ^{15}N $\bar{\sigma}$ values for the Lewis site 1 and Lewis site 2 pyridine resonances

Table II. Low Index Planes for Transition Aluminas[a]

crystal plane	layer	no. of sites/ 100 Å^2	Ia (T_d) sites	Ib (O_h) sites	IIa (T_d; O_h) sites	IIb ($2O_h$) sites	III ($3O_h$) sites
(111)	A	14.5	3.6		10.8		
	B	14.5				10.8	3.6
(110)	C	9.3	4.7			4.7	
	D	9.3		9.3			
(100)		12.5		12.5			

[a] Reproduced and corrected from ref 18.

are shielded relative to solid pyridine. The increased shielding of $\bar{\sigma}$ for each surface species is the result of a shift in one or more of the PAS elements to yield average values of increased shielding. Additionally, both resonances display values of δ and η which are reduced from that of solid pyridine. The experimental values of δ and η are the elements of "apparent" tensors, which means that they may represent either true linear combinations of the PAS elements for the surface species (this would be the case for motionless pyridines) or motionally modified resonances which would result from the linear mixing of PAS elements which are orthogonal to the axis of reorientation. The subsequent discussion of the ^2H NMR results indicates that significant anisotropic motion of coordinated pyridine is present.

The determination of the true relative pyridine populations of the two Lewis sites is crucial for the following analysis of the ^{15}N spectra. In general, a true ratio of populations is not reflected by the relative intensities of cross-polarization (CP) signals, especially when using CP pulses of arbitrary duration. This is due to the variation of cross-polarization efficiencies for nuclei as a function of chemical and motional environment. Therefore, the accurate determination of the ratio of site populations requires either the utilization of a CP pulse which enhances each signal to the same extent, or the determination of a correction factor for the relative signal intensities by independent methods. For this study, a series of ^{15}N NMR experiments was performed for each surface preparation in which the cross-polarization pulse was varied from 1 to 10 ms. Each series demonstrated a constant ratio of signal intensities for the Lewis site resonances with optimum signal enhancement for a pulse width of 3 ms. This constant ratio of relative signals indicates that the cross-polarization efficiencies for the pyridine ^{15}N nuclei are the same for both sites; hence the ratio of pyridine populations corresponds with the ratio of spectral intensities.

Considering the acidic site heterogeneity which is present on γ-alumina surfaces,[17] it is appropriate to question why the ^{15}N NMR spectra show two distinct Lewis acid sites rather than several or simply a continuous distribution of sites, which would be reflected in a single broad resonance. In an attempt to answer this question, we found the review article by Knozinger and Ratnasamy[18] to be a valuable reference. In that review, they presented a lucid description of the various surface models and site configurations based upon the consideration of an ideal surface composed of low index defect–spinel crystal planes. In the spinel lattice one can consider two such index planes which are believed to give the largest contribution to the composition of the surface, specifically the (110) and (100) planes for γ-alumina.[19] The (111) plane is believed to predominate the surface of η-alumina.[19] The cation site distribution for the various low index planes is summarized in Table II. In the (111) plane there are two types of layers, which contain different Al^{3+} cation distributions. They are designated as A and B layers. The A layer has 24 occupied Al^{3+} cation positions per 100 Å^2, 8 of which are octahedral locations, and the remaining 16 are tetrahedral interstices. The B layer also has 24 occupied cation positions, all of which are octahedral. For the (100) plane, cations reside only in octahedral

(13) Dixon, W. T.; Schaefer, J.; Sefcik, M. D.; Stejskal, E. O.; McKay, R. A. *J. Magn. Reson.* **1982**, *49*, 341–345.
(14) (a) Jakobsen, H. J.; Ellis, P. D.; Inners, R. R.; Jensen, C. F. *J. Am. Chem. Soc.* **1982**, *104*, 7442. (b) Marchetti, P. S.; Ellis, P. D.; Bryant, R. G. **1985**, *107*, 8191.
(15) Deming, S. N.; Morgan, S. L. *Anal. Chem.* **1973**, *45*, 278.
(16) Schweitzer, D.; Spiess, H. W. *J. Magn. Reson.* **1974**, *15*, 529.
(17) Majors, P. D.; Raidy, T. E.; Ellis, P. D., submitted for publication.
(18) Knozinger, H.; Ratnasamy, P. *Catal. Rev. Sci. Eng.* **1978**, *17* (1), 31–70.
(19) Lippens, B. C.; Steggarda, J. J. In *Physical and Chemical Aspects of Adsorbents and Catalysts*; Linsen, B. C., Ed.; Academic Press: New York, 1970.

interstices. The (110) plane contains a pair of layers denoted as C and D. In the C layer equal numbers of Al^{3+} cations are aligned in tetrahedral and octahedral locations, whereas for the D layer cations in octahedral interstices occur exclusively. By applying Pauling's electrostatic valence rule,[20] one can conclude that Al^{3+} cations in octahedral positions show a partial charge equal to +0.5 to each ligand, whereas those in tetrahedral positions show a partial charge of +0.75.

There are three major hydroxyl site classifications which correspond directly to the number of Al^{3+} cations to which the hydroxyl oxygen atom is coordinated. Type I hydroxyl sites are attached to only one Al^{3+} cation, type II to two, and type III to three subsurface aluminum cations.[21] Type I hydroxyl oxygens share electron density with only the Al^{3+} atom, so the site I hydroxyls are the most labile type. Type III hydroxyls are shown to be least likely to undergo desorption, and type II hydroxyls are of intermediate lability. The Lewis sites correspond with the vacancies which are generated upon desorption of the hydroxyl groups. For the lower temperature surface preparations, the majority of these hydroxyl leaving groups are probably type I groups.

Actually a maximum of only half of the surface layer cations can form anion vacancies which are available for the coordination of basic molecules. This is due to the mechanism by which these anion vacancies are generated. In this process, two neighboring hydroxyl groups combine to form a water molecule which is desorbed during surface preparation. The remaining oxygen atom occupies one of the cation sites. Consider, for example, two neighboring hydroxyl groups, type I and type II, on the A layer of the (111) plane. Since type I hydroxyl groups are more labile than the type II groups, it is probable that the desorbing water oxygen atom originates from the type I hydroxyl species.[18] This reasoning can also be extended to neighboring type II and type III sites. After the surface has been degassed above 670 °C, all adjacent hydroxyl groups have been eliminated,[11] so the site distribution for the EDA surface should give a good representation of the cation site distribution for the surface.

Since both tetrahedrally and octahedrally coordinated Al^{3+} cations can form anion vacancies on γ-alumina surfaces, it is reasonable that ^{15}N NMR can detect pyridine occupying two different Lewis acid sites. It is well-known that the chemical shift is a sensitive probe of local charge distributions. Hence, the two different partial charges could separate the ^{15}N chemical shifts for pyridine occupying two different types of Al^{3+} cation sites, i.e., the tetrahedral and octahedral anion vacancies on the surface. By using the electrostatic valence rule, the two resonances may tentatively be assigned as octahedral (O_h) and tetrahedral (T_d) species for the most and least shielded resonances, respectively.

A trend which is readily apparent in the ^{15}N spectra is the variation of the relative contributions of the two resonances as a function of surface preparation. Approximately 61% of the coordinated pyridine resides in tetrahedral surface sites for the PDA sample, a 57% tetrahedral site occupation for the IDA sample, and 51% tetrahedral site population for pyridine on the EDA surface (see Table I). Considering the information available (see Table II[22]) for the cation site distributions for the various γ-alumina crystal planes,[18] it may be feasible to use the experimentally observed surface T_d and O_h site pyridine populations to determine the relative contributions of the various crystal planes to the composition of the surface. Secondly, the dependence of the acid site distribution upon the surface preparation conditions might give further information about the composition of the surface.

The surface of γ-alumina has been proposed to be composed mainly of the (110) plane.[19] If the surface were composed exclusively of this plane, we calculate from the data in Table II that equal amounts of type I tetrahedral (Ia) and octahedral (Ib) anion vacancies would arise (assuming that all of the C layer IIb sites are left with oxygen atoms by the desorbing Ia hydroxyls, and half of the D layer Ib sites are covered by oxygen atoms after the combination with neighboring Ib sites). Assuming the same lability for Ia and Ib hydroxyls, the distribution of T_d to O_h anion vacancies would remain at 50% for the entire range of surface preparation temperatures. At this hypothetical extreme, all surface hydrogens will have been desorbed. For a surface which is composed of (100) planes, only type Ib (O_h) hydroxyl groups exist. Therefore, only octahedral anion vacancies can exist on the (100) plane.

For a surface composed exclusively of the (111) plane, the information in Table II predicts an overwhelming majority of tetrahedral sites for low-temperature surface preparations because all type I sites are Ia (T_d). With higher surface preparation temperatures, the distribution of T_d to O_h anion vacancies for this plane also converges to 50% for both species. This calculation assumes that half of the remaining type IIa hydroxyls on the A layers are desorbed. (Type IIa sites are composed of both T_d and O_h coordinatively unsaturated cations. For this calculation, we consider the IIa vacancies as effectively tetrahedral by virtue of the larger partial electrostatic charge,[20] and also the lower steric obstruction for the tetrahedrally vs. the octahedrally coordinated cation.) Further, this calculation assumes that on the B layers a number of type IIb hydroxyls which is equal to the number of type III sites are desorbed and that half of the remaining type IIb hydroxyls are desorbed.

Consider a surface which is composed of equal areas of (110) and (100) index planes. Upon the removal of as many type I hydroxyls as possible, the average surface anion vacancy site density is approximately four sites per 100 Å^2, 30% of which are tetrahedral. Assuming that all of the C layer type II sites have been closed by desorbing Ia hydroxyl groups, the distribution of T_d and O_h sites would show no variation with higher surface preparation temperatures as the desorption of waters will be complete at lower surface preparation temperatures. Consider next a surface composed of equal contributions from the (111) and (110) index planes. After the removal of as many type I hydroxyls as possible, the average surface anion vacancy site density is approximately four sites per 100 Å^2, 64% of which are tetrahedral cation sites. At higher surface preparation temperatures, the additional generation of as many type II anion vacancies as is possible yields an overall average surface density of approximately six sites per 100 Å^2; and a distribution of 50% for both T_d and O_h anion vacancies.

The model of the surface which is composed of (111) and (110) planes in equal proportions tentatively shows good agreement with the experimental results. The calculated 64% tetrahedral anion vacancy for the 1:1 surface compares closely with the 61% tetrahedral site pyridine population which is observed for the PDA sample (Table I). Both experiment (EDA sample) and model indicate an approximate 50% tetrahedral site distribution at elevated surface preparation temperatures. This result is in conflict with previous studies which suggest that the combination of (110) and (100) planes gives a better description of γ-alumina surfaces.[19]

The (110) and (100) combination calculates a majority of O_h anion vacancies, which is apparently in disagreement with the experimental results. Since the interpretation of the experimental results depends upon the tentative assignments of the Lewis resonances, one might suspect an error in these assignments (i.e., a reversed assignment of the T_d and O_h resonances). However, the calculated distribution for the combination of (110) and (100) planes fails to match the experimental distribution in surface preparation temperature dependence; specifically it displays no surface preparation temperature dependence at higher temperatures, and it deviates significantly from the approximately 50:50 population ratio for T_d:O_h which is experimentally observed at higher temperatures.

(20) Pauling, L.; Pauling, P. In *Chemistry*; W. H. Freeman: San Francisco, 1975; Chapter 18–2, p 394.

(21) Type I and II groups are further classified according to the coordination number for the Al^{3+} cations, yielding a total of five types of hydroxyl sites. These sites have been assigned to the five vibrationally distinct hydroxyl species observed on γ-alumina.

(22) Table II is a corrected reproduction of Table IV from ref 18. The correction merely involves the exchange of labels Ia and Ib, and IIa with IIb so that the table is consistent with the text of ref 18.

To make any firm conclusions concerning the structure of the γ-alumina by this technique, a more detailed study involving variable pyridine surface concentration and a larger range of surface preparation conditions would be necessary. It should be kept in mind that the previous analysis is idealized, for it is known that alumina surfaces undergo some degree of re-formation, especially at higher temperatures, resulting in, e.g., the regeneration of labile hydroxyl species, cationic migration, etc. The rearrangement of bulk and surface structure of transition aluminas is known to occur at elevated temperatures resulting in the lowering of surface strain. The transition temperature for these aluminas to the inert α-alumina is approximately 910–950 °C and involves the migration of the cations into exclusively octahedral interstices.[18] A substantial surface strain could cause the mobilization of surface atoms at lower temperatures.[11] This surface re-formation process may also explain the presence of a shift in the Lewis site 1 isotropic resonance toward that for the site 2 resonance with increasing surface degassing temperature (see Table I). An alternative explanation to the resonance shift is the observation of pyridine appearing at multicenter (types II and III) anion vacancies, where two or three cations are exposed.

A series of hydration experiments for pyridine-^{15}N on PDA was performed in which exposure of the surface to air led to the observation of a change in the ^{15}N spectra. When one of the end caps of the NMR sample rotor was removed and allowed to stand in air for 4.5 h, the ^{15}N cross-polarization spectrum displayed a new resonance of diminished intensity but appreciable anisotropy which developed in exclusion of the two original resonances. This tensor has an isotropic shift of −110 ppm, which falls near the range of the Lewis site I resonance. This suggests the formation of a different coordination environment, possibly involving the modification of one binding site and the closing of another completely (water is known to displace pyridine on alumina surfaces[11]). In a second sample, the pyridinated surface was removed from the NMR sample rotor and exposed to air for 30 min. This sample was returned to the rotor and rerun to show a single resonance at −78 ppm. This resonance was obtainable only by Bloch decays (cross-polarization was shown to be ineffective for a large range of contact times) and demonstrated isotropic reorientation as evidenced also by the invariance of the spectrum to the presence or absence of magic angle spinning. The chemical shielding of this surface species is in close agreement with the value reported for the physisorbed and hydrated species given in the previous study.[3] Presumably the pyridine is being displaced from the surface by saturating amounts of water being adsorbed during exposure.

Although the ^{15}N MAS spectra for pyridine on these dehydroxylated aluminas indicate the presence of two chemically distinct Lewis-type coordination environments, it is evident that a distribution of some type exists for each of these coordination environments. This is displayed in the varying line widths (Table I) and also by the minor but observable mismatch of the MAS simulations with the corresponding experimental line shapes (both the variation in line width and the line-shape mismatch may also be attributed at least partially to the dipolar coupling of the ^{15}N nucleus of pyridine to the quadrupolar ^{27}Al ($I = {}^5/_2$) surface cation). Pyridine has previously been reported to form sterically inequivalent surface species on aluminas[23] which involves the interaction with surface anions. This steric heterogeneity is also manifested in the motionally averaged solid-state ^2H NMR spectra of di-ortho-deuterium-labeled pyridine.

The wide-line ^2H magnetic resonance spectra for pyridine-α,α'-d_2 on PDA γ-alumina show a line shape with nondistinct discontinuities (Figure 3a). Comparison of this line shape with the quadrupolar spin–echo spectral simulation of an α site deuteron on stationary pyridine (Figure 3d) shows that significant motional narrowing of the resonance has taken place. The experimental line shape is shown by experimentation to be independent of the echo delay value, indicating that the reorientational motion is in the limit of fast exchange (i.e., the reorientational exchange rate is greater than the vibrationally averaged ^2H quadrupolar splitting for a pyridine deuteron $\omega_Q/2\pi$ which is 133.5 kHz[24]).

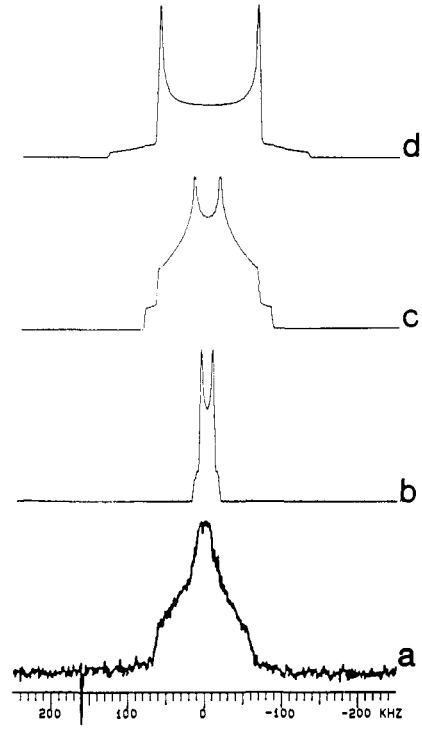

Figure 3. (a) 61-MHz ^2H quadrupolar spin–echo spectrum of pyridine-α,α'-d_2 on γ-alumina (PDA surface, 25% monolayer surface coverage): 32 000 0.5-s repetitions, 40-μs quadrupolar echo delay; 90° pulse width = 3.0 μs. (b) Quadrupolar spin–echo spectral simulation of a pyridine molecule executing rapid continuous diffusion about its twofold symmetry axis. (c) Quadrupolar spin–echo spectral simulation of a pyridine molecule executing rapid two-site jumps about its symmetry axis. (d) Quadrupolar spin–echo spectral simulation of a stationary pyridine molecule.

The motion of pyridine on the PDA surface is seen to be more complicated than the performance of continuous diffusion or rapid twofold site jumps about the C_2 axis of pyridine, as evidenced by spectral simulation of the motional models (Figure 6, b and c, respectively).[25] There is, however, apparently a significant contribution from both modes of reorientation in the experimental line shape. In a previous ^{13}C NMR study[2] of pyridine on γ-alumina, the decrease in cross-polarization efficiency of the C_γ carbon relative to that of the C_α and C_β carbons indicated C_2 axis reorientation (the same phenomenon has been reported for pyridine on silica–aluminas[27]). This motion causes the modulation of the C_γ–H_γ and/or the H_γ–H dipolar interactions, the basic interactions which are necessary for cross-polarization.

The nondistinct nature of the ^2H line shapes shows that more than two motional species are present, but that in actuality a heterogeneous distribution of motional Lewis species probably exists for each of the Lewis sites. This heterogeneity arises because of steric variations (the variation in binding site accessibility), the contribution of the various crystal planes (including higher order index planes) to the surface structure,[18] surface discontinuities, lateral interactions with hydroxyl groups,[12] and surface defects (energetically unfavorable atomic arrangements).[18] In general, the consideration of the surface structure as an abrupt termination of the bulk crystalline structure is a rough approximation for energetic reasons, and some atomic rearrangement would take

(23) Knozinger, H.; Stolz, H. *Fortschrittsber. Kolloide Polym.* **1971**, *55*, 16.

(24) Barnes, R. G.; Bloom, J. W. *J. Chem. Phys.* **1972**, *57*, 3082.

(25) Such aromatic ring dynamics have been previously studied in detail by Opella et al.[26]

(26) Gall, C. M.; DiVerdi, J. A.; Opella, S. J. *J. Am. Chem. Soc.* **1981**, *103*, 5039–5043.

(27) Maciel, G. E.; Haw, J. F.; Chuang, I.-S.; Hawkins, B. L.; Early, T. A.; McKay, D. R.; Petrakis, L. *J. Am. Chem. Soc.* **1983**, *105*, 5529–5535.

place at a real surface in order to minimize surface strain.

Pyridine is seen to have a fortuitous combination of properties which make for an excellent probe of alumina surfaces. Firstly, its low basicity allows for the exclusive observation of Lewis acid sites. Secondly, the sensitivity of the ^{15}N chemical shift for pyridine is sufficient to resolve the different Lewis sites. Finally, the large size (relative to, e.g., NH_3) of the pyridine ring and the conformational restrictions which are imposed upon its constituent atoms allows for the study of the steric properties of the binding site. The site-selective pyridine is seen to be especially informative when used in conjunction with the nonselective ammonia probe molecule,[17] which allows for the study of Brønsted and Lewis acid site distributions on these alumina surfaces.

The present study illustrates how high-field solid-state ^{15}N and ^{2}H NMR spectroscopies can provide new structural insights about the nature of nitrogen Lewis acid/base adducts on γ-alumina surfaces, and possibly the morphology of these surfaces as well. In future work we will examine the possibility of positively identifying each ^{15}N resonance to the appropriate type of cation site by examining a variety of types of aluminas where the cation site occupancy will differ from γ-alumina. If this hypothesis is supported by further experiments, ^{15}N NMR may prove to be a very useful method for determining the distribution of tetrahedral vs. octahedral sites on various alumina surfaces, a number which is difficult to obtain by other methods.

Acknowledgment. The authors wish to acknowledge support from the National Science Foundation via Research Grant CHE 83-06580 and access to the Regional Instrument Facility at the University of South Carolina which is supported by the NSF, Grant CHE 8207445.

Registry No. Al_2O_3, 1344-28-1; pyridine, 110-86-1.

Theoretical Study of the Ammoniated NH_4 Radical and Related Structures

E. Kassab* and E. M. Evleth

Contribution from Dynamique des Interactions Molêculaires, E.R. 271, Tour 22, Universitê Pierre et Marie Curie, 75230 Paris, France. *Received May 19, 1986*

Abstract: The ground- and some of the excited-state surfaces for the reaction of the Rydberg radical NH_4 to give either $NH_3 + H$ or $NH_2 + H_2$ are computed. The preferred ground reaction channel is that observed experimentally, the formation of $NH_3 + H$. The Rydberg character, as well as the low barrier for fragmentation, is rationalized using a Rydberg extended-state structure correlation diagram. The excited-state surfaces show deep potential wells whose forms are also rationalized using this correlation diagram. Calculations on the surface of tetramethylammonium radical show no enhanced stability due to alkyl substitution. Comparative calculations on the complexation energies of $NH_4^+(NH_3)_n$ and $NH_4(NH_3)_n$, $n = 1$-6, show the semiionic character of the Rydberg radical. The variation of stepwise complexation energies with n for the Rydberg species is not completely understood. The stability of solvated NH_4 radical in liquid NH_3 is estimated to be of the same order as $(NH_4^+)_s + (e^-)_s$.

Recently, Gellene, Porter, and co-workers[1] have observed the formation of a series of ammoniated NH_4 radical species, $NH_4(NH_3)_n$, $n = 1, 3$. These species are generated in molecular beams by electron addition to the $NH_4^+(NH_3)_n$ cationic species. The existence of $NH_4(NH_3)_n$ species takes on special interest since the parent radical, NH_4, has not yet been observed in the ground state.[2] Additional interest occurs because this and the H_3 species represent the first characterized members of a broad class of materials referred to as Rydberg radicals. The D_3O radical and the H_3O–water complexed species have also been detected.[3] Although NH_4 was first well characterized by emission,[2a] the existence of mercury amalgams of ammonium and alkylammonium radicals has long been known.[4] The possible condensed-phase existence of ammonium radicals formed by electron capture by ammonium ions is suggested by a number of experimental observations.[5] We have recently proposed[6] the generation of ammoniated NH_4 radicals in the photodecomposition of ammonia and water–ammonia clusters.

If Rydberg radicals exist as complexes or solvated species in the condensed phase, as they do in small clusters, a conceptual problem arises in describing their diffuse electronic structures in the presence of large numbers of other molecules.[7] Even the electronic structure description of the isolated NH_4 species represents a conceptual problem in valence orbital terms. Originally, Mulliken recognized the possible Rydberg character of this radical.[8] Herzberg anticipated[9] the NH_4 radical as a member of

(1) (a) Gellene, G. I.; Porter, R. F. *J. Phys. Chem.* **1984**, *88*, 6680–6684. (b) Jeon, S.; Raksit, J. A. B.; Gellene, G. I.; Porter, R. F. *J. Am. Chem. Soc.* **1985**, *107*, 4129–4133.

(2) (a) Herzberg, G. *Faraday Discuss. Chem. Soc.* **1981**, *71*, 163–173. (b) Whittaker, E. A.; Sullivan, B. J.; Bjorklund, G. C.; Wendt, H. R.; Hunziker, H. J. *J. Chem. Phys.* **1984**, *80*, 961–962.

(3) Gellene, G. I.; Porter, R. F. *J. Chem. Phys.* **1984**, *81*, 5570–5576.

(4) For a review up until 1968, see: (a) Wan, J. K. S. *J. Chem. Educ.* **1968**, *45*, 40–43. Since 1968, see: (b) Kariv-Miller, E.; Nanjundiah, C.; Eaton, J.; Swenson, K. E. *J. Electroanal. Chem.* **1984**, *167*, 141–155. (c) Littlehailes, J. D.; Woodhall, B. J. *Faraday Discuss. Chem. Soc.* **1968**, *45*, 187–192.

(5) (a) Anbar, M. "Solvated Electron", *Adv. Chem. Ser.* **1965**, *No. 50*, 55–81, and references cited therein. (b) Horner, L. "Organic Electrochemistry"; Baizer, M. M., Ed.; Marcel Dekker: New York, 1973; pp 429–443. (c) Brooks, J. M.; Dewald, R. R. *J. Phys. Chem.* **1971**, *75*, 986–987. (d) Brown, O. R. *Electrochemistry* **1974**, *4*, 55–77. (e) Quinn, R. K.; Lagowski, J. J. *J. Phys. Chem.* **1968**, *72*, 1374–1378. (f) Dye, J. L.; DeBacker, M. G.; Dorfman, L. M. *J. Chem. Phys.* **1970**, *52*, 6251–6258. (g) Laitinen, H. A.; Nyman, C. J. *J. Am. Chem. Soc.* **1948**, *70*, 3002–3008. (h) Gedye, R. N.; Sadana, Y. N.; *J. Org. Chem.* **1980**, *45*, 3721–3722 and references cited therein.

(6) (a) Cao, H. Z.; Kassab, E.; Evleth, E. M. *J. Chem. Phys.* **1984**, *81*, 1512. (b) Evleth, E. M.; Cao, H. Z.; Kassab, E. *Photochemistry and Photophysics above 6 eV*; Lahmani, F., Ed.; Elsevier: Amsterdam, 1985; pp 479–495.

(7) (a) For a discussion of high-pressure and condensed-phase effects on Rydberg spectra, see: Robin, M. B. *Higher Excited States of Polyatomic Molecules*; Academic Press: New York, 1974; Vol. I, pp 76–91. (b) Gaathon, A.; Jortner, J. *Can. J. Chem.* **1977**, *55*, 1801. (c) Messing, I.; Raz, B.; Jortner, J. *Chem. Phys.* **1966**, *4*, 4470. (d) Evleth, E. M.; Gleghorn, J. T. *Chem. Phys. Lett.* **1983**, *94*, 373–376.

0002-7863/87/1509-1653$01.50/0 © 1987 American Chemical Society